

Co-phased 360-degree profilometry of discontinuous solids with 2-projectors and 1-camera

Manuel Servin, Guillermo Garnica and J. M. Padilla.

Centro de Investigaciones en Optica A. C., 115 Loma del Bosque, 37150 Leon Guanajuato, Mexico
mservin@cio.mx , garnica@cio.mx , moises@cio.mx .

Abstract: Here we describe a co-phased 360-degree fringe-projection profilometer which uses 2-projections and 1-camera and can digitize discontinuous solids with diffuse light surface. This is called co-phased because the two phase demodulated analytic-signals from each projection are added coherently.

OCIS codes: (120.0120) Instrumentation, measurement, and metrology; (120.5050) Phase measurement.

1. Introduction

One sided or 180-degree fringe projection profilometry using phase-demodulation techniques is well known since the classical paper by Takeda et al. in 1982 [1]. However to obtain a full 360-degree profilometer one needs to position the solid over a turntable to have access to all solid perspectives. Previous efforts have mainly concentrated in digitizing very smooth, quasi-cylindrical objects [2]. This is because smooth, quasi-cylindrical solids are easier to digitize with previous 360-degree profilometers. Here we are proposing a co-phased 2-projector, 1-camera 360-degree profilometer which is capable to digitize highly discontinuous 3D solids. This co-phased 2-projectors, 1-camera profilometer is a blending of two previous published techniques by the same authors [3,4]. We have digitized a human skull model all around it (360-degrees). The digitizing of this plastic skull shows the 3D digitizing capabilities of this profilometer to digitize discontinuous non-convex 3D solids.

2. Co-phased 180-degree fringe-projection profilometry using 2-projectors and 1-camera

The left- L and right- R projected fringes as seen by the CCD camera are given by,

$$\begin{aligned} I_L(x, y, \alpha) &= a_L(x, y) + b_L(x, y) \cos[\omega_0 x - g z(x, y) + \alpha]; \quad \omega_0 = \nu_0 \cos(\varphi_0), \quad g = \tan(\varphi_0), \\ I_R(x, y, \alpha) &= a_R(x, y) + b_R(x, y) \cos[\omega_0 x + g z(x, y) + \alpha]; \quad \alpha \in \{0, \pi/2, \pi, 3\pi/2\}. \end{aligned} \quad (1)$$

Where the digitizing object is $z = z(x, y)$ and $\alpha \in \{0, \pi/2, \pi, 3\pi/2\}$ are the 4 phase-steps used.

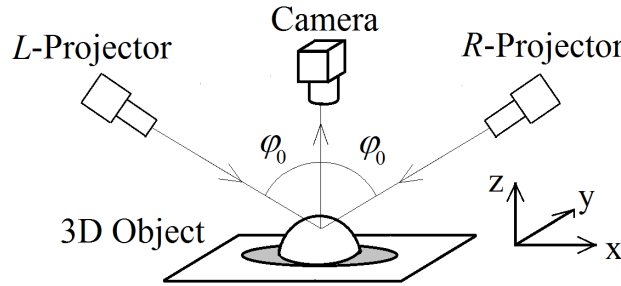


Figure 1. Co-phased 180-degree fringe-projection profilometer with 2-projectors and 1-camera [3].

We then use a 4-step phase-shifting demodulation algorithm for both projected images as,

$$\begin{aligned} A_L(x, y) e^{i g z(x, y)} &= I_L(0) + I_L(\pi/2) e^{i \pi/2} + I_L(\pi) e^{i \pi} + I_L(3\pi/2) e^{i 3\pi/2}, \\ A_R(x, y) e^{-i g z(x, y)} &= I_R(0) + I_R(\pi/2) e^{i \pi/2} + I_R(\pi) e^{i \pi} + I_R(3\pi/2) e^{i 3\pi/2}. \end{aligned} \quad (2)$$

These two analytic signals in Eq. (2) have complementary shadows and their digital co-phased sum is,

$$\begin{aligned} A_{L+R}(x, y) e^{i g z(x, y)} &= A_L(x, y) e^{i g z(x, y)} + [A_R(x, y) e^{-i g z(x, y)}]^*, \\ A_{L+R}(x, y) e^{i g z(x, y)} &= [A_L(x, y) + A_R(x, y)] e^{i g z(x, y)}. \end{aligned} \quad (3)$$

The analytic signal $A_{L+R}(x, y) \exp[i g z(x, y)]$ therefore has no shadows cast by $z(x, y)$ as seen by the camera.

3. Co-phased 360-degree fringe projection profilometry with 2-projectors and 1-camera

The co-phased 2-projectors 1-camera, 360-degree ($\varphi \in [0, 2\pi)$) profilometer set-up is shown in Fig. 2,

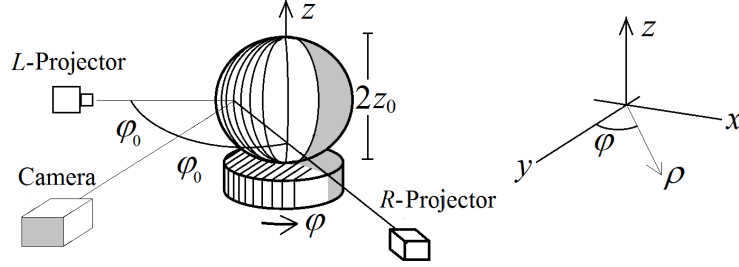


Fig. 2. Co-phased 360-degree profilometer with 2-projectors and 1-camera to digitize discontinuous objects $\rho = \rho(z, \varphi)$.

For each rotation step φ we grab the central column CCD pixels of the solid $\rho = \rho(z, \varphi)$, $z \in [-z_0, z_0]$, $\varphi \in [0, 2\pi)$. We then use a 4-step phase-shifting algorithm to phase-demodulate their analytic signals,

$$\begin{aligned} A_L(z, \varphi) e^{i g \rho(z, \varphi)} &= I_L(0) + I_L(\pi/2) e^{i \pi/2} + I_L(\pi) e^{i \pi} + I_L(3\pi/2) e^{i 3\pi/2}, \\ A_R(z, \varphi) e^{-i g \rho(z, \varphi)} &= I_R(0) + I_R(\pi/2) e^{i \pi/2} + I_R(\pi) e^{i \pi} + I_R(3\pi/2) e^{i 3\pi/2}. \end{aligned} \quad (4)$$

Their digital co-phased sum is defined everywhere because they have complementary shadows,

$$\begin{aligned} A_{L+R}(z, \varphi) e^{i g \rho(z, \varphi)} &= A_L(z, \varphi) e^{i g \rho(z, \varphi)} + [A_R(z, \varphi) e^{-i g \rho(z, \varphi)}]^*, \\ A_{L+R}(z, \varphi) e^{i g \rho(z, \varphi)} &= [A_L(z, \varphi) + A_R(z, \varphi)] e^{i g \rho(z, \varphi)}; \quad z \in [-z_0, z_0], \varphi \in [0, 2\pi]. \end{aligned} \quad (5)$$

4. Experimental results

Fig. 3 show the images from the left and the right projectors; generating left and right shadows at the discontinuities

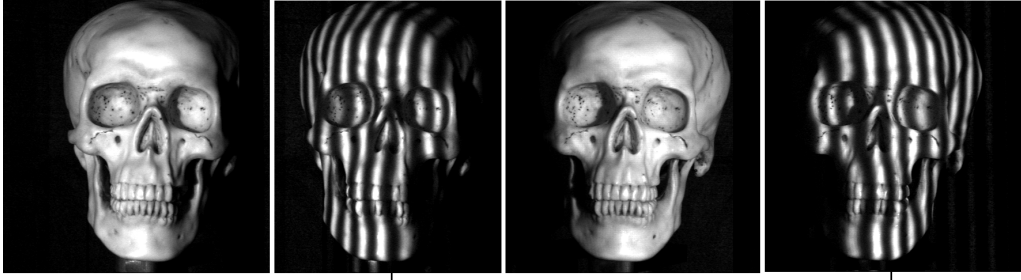


Fig. 3. The digitizing plastic skull from the left and right illumination perspectives

The two 4-step phase-shifted algorithms used to demodulated the 2 analytic signal perspectives are,

$$\begin{aligned} A_L(z, \varphi) e^{i g \text{Skull}(z, \varphi)} &= I_L(0) + I_L(\pi/2) e^{i \pi/2} + I_L(\pi) e^{i \pi} + I_L(3\pi/2) e^{i 3\pi/2}, \\ A_R(z, \varphi) e^{-i g \text{Skull}(z, \varphi)} &= I_R(0) + I_R(\pi/2) e^{i \pi/2} + I_R(\pi) e^{i \pi} + I_R(3\pi/2) e^{i 3\pi/2}. \end{aligned} \quad (6)$$



Fig. 4. Binary masks of good fringe-contrast for the left, right and sum of the analytic signals in Eqs. (6) and (7).

Now let us sum the two co-phased analytic signals from the left and the right projections in Eq. (6).

$$\begin{aligned} A_{L+R}(z, \varphi) e^{i g \text{Skull}(z, \varphi)} &= A_L(z, \varphi) e^{i g \text{Skull}(x, y)} + [A_R(z, \varphi) e^{-i g \text{Skull}(z, \varphi)}]^*, \\ A_{L+R}(z, \varphi) e^{i g \text{Skull}(z, \varphi)} &= [A_L(z, \varphi) + A_R(z, \varphi)] e^{i g \text{Skull}(x, y)}; \quad z \in [-z_0, z_0], \varphi \in [0, 2\pi]. \end{aligned} \quad (7)$$

The two analytic signals in Eq. (6) have complementary shadows at the skull discontinuities, but their co-phased sum $A_{L+R}(x, y) \exp[i g \rho(z, \varphi)]$ in Eq. (7) has no one (see Fig. 4).

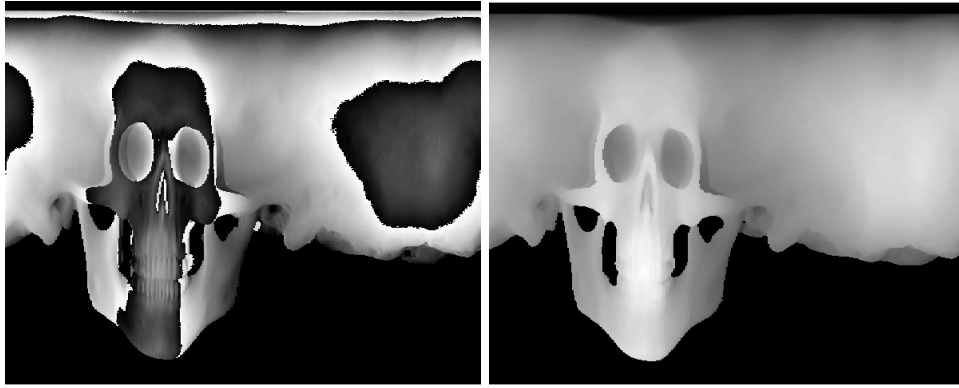


Fig. 5. Wrapped and unwrapped phase of the co-phased sum in Eq. (7) in flat cylindrical-coordinates.

Finally Fig. 6 shows the 2 rendering 3D-perspectives of the digitized plastic skull.

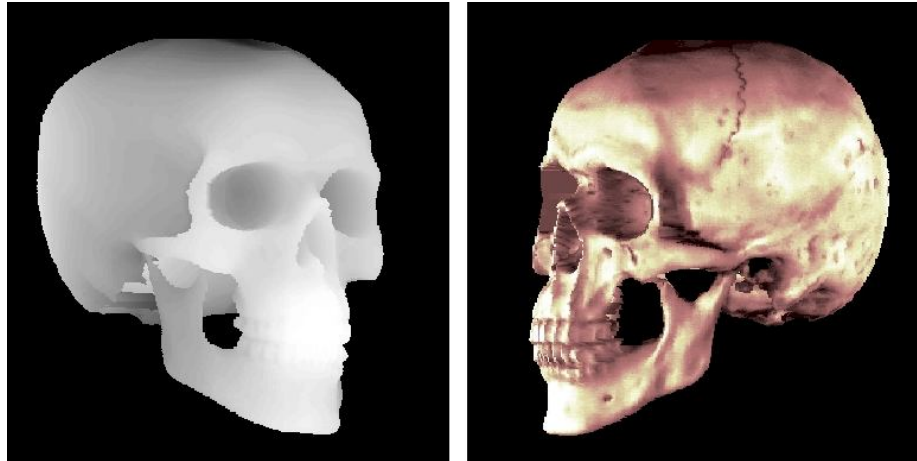


Fig. 6. The left panel shows the 3-dimensional rendering of the plastic skull in gray-level phase-values.
The right panel shows another skull perspective with the magnitude of the fringes superimposed.

5. References

- [1] M. Takeda, H. Ina, S. Kobayashi, "Fourier-transform method of fringe-pattern analysis for computer-based topography and interferometry," J Opt. Soc. Am. A 72, 156–60 (1982).
- [2] M. Halioua, R. S. Krishnamurthy, H. C. Liu, and F.P. Chiang, "Automated 360o profilometry of 3-D diffuse objects," Appl. Opt. 24, 2193-2196 (1985).
- [3] M. Servin, G. Garnica, J. C. Estrada, and J. A. Quiroga, "Coherent digital demodulation of single-camera N-projections for 3-D object shape measurement: Co-phased profilometry," Opt. Exp. 21, 24873-24878 (2013).
- [4] M. Servin, G. Garnica, J. C. Estrada, and J. M. Padilla, "High-resolution low-noise 360-degree digital solid reconstruction using phase-stepping profilometry," Opt. Exp. 22, 10914-10922 (2014).